


Cite this: *RSC Adv.*, 2024, 14, 38689

A general synthesis method for small-size and water-soluble NaYF₄:Yb, Ln upconversion nanoparticles at high temperature†

Mingda Liu,^{‡a} Jianwen Xu,^{‡a} Kai Zhu,^a Ming Yan,^{*a} Min He,^b Xiaowei Huang,^b Yan Xu,^b Wei Wang,^{*c} Shibo Zhao^d and Qinghui Zeng^{ib} ^{*ab}

In this work, we developed a general synthesis method for the water-soluble lanthanide ion-doped NaYF₄ upconversion (UC) nanoparticles (NPs) using triethylene glycol (TEG) as a high temperature solvent and diacid as a surfactant. Since the boiling point of the TEG is as high as 289.4 °C, the synthesis temperature can be correspondingly increased to a higher temperature that is a bit lower than this one. Therefore, water-soluble UCNPs with a small size (<50 nm) can be easily prepared. The nanocrystal growth temperature could be elevated from 180 °C to 285 °C due to the superiority of the high-temperature polar solvent environment introduced in this work. The temperature-dependent nanocrystal growth mechanism and luminescent properties of UCNPs are deeply explored. Different chain length diacids, e.g., three-carbon chain length propanedioic acid (PDA), six-carbon chain length hexanedioic acid (HDA) and nine-carbon chain length azelaic acid (AA), were used in this work to prepare the water-soluble UCNPs in polar solution, and we finally found that the fluorescent intensity and water-stability are inversely proportional to the carbon chain length of the ligand. PDA was proved to be an optimum surfactant to prepare the most stable water-soluble UCNPs. As a result, the water-soluble UCNPs we prepared can also be successfully applied in the upconversion luminescent cell imaging. This study opens up new avenues for the synthesis of water-soluble UCNPs with small sizes and provides more opportunities for their applications in fields such as biological imaging and biological detection.

Received 22nd October 2024
Accepted 25th November 2024

DOI: 10.1039/d4ra07543a

rsc.li/rsc-advances

1. Introduction

Lanthanide ion (Ln)-doped upconversion (UC) luminescent nanoparticles (NPs) have received considerable attention owing to their wide applications in photoelectronic devices, bioimaging, photodynamic therapy and catalysis.^{1–5} Compared with the traditional organic dyes and quantum dots, UCNPs have many advantages, including narrower emissive band, longer

luminescent lifetime, higher chemical stability, lower toxicity to cells and lower biological auto-fluorescence under near-infrared excitation.⁶ All these advantages make UCNPs an ideal luminescent candidate in bio-applications.^{7,8} However, the biological environments require the UCNPs to be biocompatible and as small as possible in dimensional size.^{9,10}

The traditional Ln-doped UCNPs synthesized in polar solvent often utilize an autoclave for hydrothermal treatment to elevate the boiling point of water as well as the growth temperature in order to obtain the relatively high luminescent UCNPs with higher crystallinity, where the citric acid or the polyethylenimine (PEI) molecule are often used as the surfactant.^{11–13} However, the lower boiling point of citrate acid (~175 °C, almost decomposes at this temperature or higher) makes it impossible to be used as a surfactant at higher temperatures (e.g., ≥180 °C) since it is well known that the highly efficient UCNPs must be prepared at a relatively high temperature, e.g., over 200 °C.¹⁴ The harsh ligand requirement and the higher temperature conditions make this traditional experiment unsuitable to prepare UCNPs at higher temperatures, thus hampering their advantages in wide production. On the other hand, thermal dynamic growth is the traditional direct synthesis method for water-soluble UCNPs with high monodispersity in polar condition; as a result, increasing the temperature tends to yield large size NPs in the sub-micrometer

^aChangchun University of Chinese Medicine, Bo Shuo Road 1035, Changchun 130117, P. R. China. E-mail: mingyan.ccucm@outlook.com; zengqinghui96000@163.com

^bNortheast Asian Institute of Traditional Chinese Medicine, Changchun University of Chinese Medicine, Bo Shuo Road 1035, Changchun 130117, P. R. China

^cDepartment of Neurosurgery, The First Hospital of Jilin University, Changchun 130000, P. R. China. E-mail: wangv@jlu.edu.cn

^dMedicine and Information College, Changchun University of Chinese Medicine, Changchun 130117, P. R. China

† Electronic supplementary information (ESI) available: Fig. S1 shows the XRD results of NaYF₄:Yb, Er NPs prepared at 180 °C, 240 °C, and 285 °C. Scheme S1 shows the traditional phase transferring of the UCNPs prepared originally in the oil phase using HDA as a substitutional ligand. Fig. S2 is the time evolution of the room-temperature UC luminescent spectra and 803 nm emission intensity of NaYF₄:20%Yb, 2%Tm NPs obtained by the phase transfer of the original oil phase UCNPs under natural position to compare the stability of the NPs. See DOI: <https://doi.org/10.1039/d4ra07543a>

‡ These authors contributed equally to this work.



range,^{12,13,15} and the small size NPs are often accompanied by large hydrodynamic diameters due to the undesired aggregation phenomena. The large size and aggregation of the resulting NPs in turn restrict the further applications of these NPs in many fields, especially in the biological cell imaging experiments.

To date, the smaller size UCNPs are usually prepared in the oil phase with 10–100 nm diameter, and the obtained UCNPs must be transferred into an aqueous solution before the biological applications through ligand exchange or polymer encapsulation.^{16,17} During the past few years, researchers have utilized hexanedioic acid (HDA), aminoethylphosphonic acid (AEP), and polymers (*e.g.*, polyacrylic acid) as hydrophilic reagents to transfer the organic phase UCNPs to the aqueous phase, which is able to functionalize the UCNPs with different surface groups simultaneously.^{18–20} However, the existing process is complicated: the UCNPs must be synthesized in the oil phase firstly and then transferred into the polar solution. It is thus impossible to avoid the following drawbacks: firstly, the obtained nanomaterials are inclined to possess poor water-solubility due to the postnatal surfactant mastered at a relatively lower temperature than the original treating process, leading to unstable experiments with the following; secondly, the polymer encapsulation and the ligand exchange-induced aggregation phenomena often lead to an increase in the hydrodynamic size of the resulting NPs; thirdly, the reduplicative purification and centrifugation process will often lead to a lower transferring efficiency of the UCNPs. As a result, ligand exchange experimental control will sacrifice the original properties of the oil phase NPs and prejudice the further bio-applications. With the enhanced applications of the UCNPs, water-soluble UCNPs with smaller size (≤ 50 nm) have become one of the focuses in the scientific community. The requirement of high temperature polar solvent and surfactant allows the direct synthesis of the resulting water-soluble UCNPs in a polar solution, which is preferable to the traditional UCNPs obtained by the phase transfer procedures. Fortunately, the relatively higher boiling point of most diacids makes them appropriate surfactant candidates to prepare water-soluble UCNPs at

a higher temperature. Table 1 lists some physical parameters; the above conclusions could be easily obtained from this table.

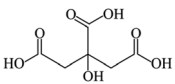
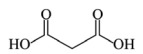
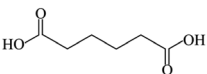
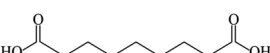
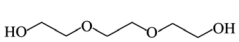
In this work, we have developed a general synthesis method for the lanthanide ions-doped NaYF₄ UCNPs using triethylene glycol (TEG) as a higher temperature solvent and diacid as a surfactant. Since the boiling point of the TEG is as high as 289.4 °C, the synthesis temperature can be correspondingly increased to a higher temperature slightly lower than 289.4 °C (*e.g.*, 285 °C). As a result, the water-soluble UCNPs with small size (<50 nm) can be easily prepared and applied in biological applications, *e.g.*, upconversion luminescent imaging. The nanocrystal growth temperature could be elevated from 180 °C to 285 °C due to the superiority of the high temperature polar solvent environment introduced in this work. The temperature-dependent nanocrystal growth mechanism and luminescent properties of UCNPs are deeply explored. The different chain length diacids, *e.g.*, three-carbon chain length propanedioic acid (PDA), six-carbon chain length hexanedioic acid (HDA) and nine-carbon chain length azelaic acid (AA) were used in this work to prepare the water-soluble UCNPs in polar solution, and we finally found that the water-stability is inversely proportional to the carbon chain length of the ligand. Propanedioic acid proved to be the optimum surfactant in this work to prepare the most stable water-soluble UCNPs. The analysis results from field-emission scanning electron microscopy (FESEM), X-ray powder diffraction (XRD), and upconversion photoluminescence (PL) spectra indicate that the synthesis of water-soluble NPs using our method is feasible and the optimal nanocrystal growth temperature is 285 °C. At the same time, the optimal surfactant is the short chain diacid molecule. The minimum size of the prepared UCNPs was 9 nm, which could be obtained through the gradient centrifugation technique.

2. Experimental section

2.1 Chemicals

The lanthanide chlorides were purchased from Aldrich in the highest purity available (>99.9%). Propanedioic acid (99%),

Table 1 Structural formula, boiling point (b.p.), relative density and solubility of different polar solvents and surfactants

	Structural formula	b.p.	Relative density	Solubility
Citric acid		175 °C, decompose at this temperature	1.67	Soluble in water, ethanol, and acetone, insoluble in diethylether and benzene, slightly soluble in chloroform
Propanedioic acid		386.8 °C (101.3 kPa)	1.63	Soluble in water, ethanol, and diethylether
Hexanedioic acid		332.7 °C (101.3 kPa)	1.36	Soluble in hot water, ethanol and diethylether organic solvent, <i>etc.</i> , slightly soluble in cold water
Azelaic acid		286.5 °C (13.3 kPa)	1.03	Soluble in hot water, ethanol and diethylether, slightly soluble in cold water
Triethylene glycol		289.4 °C (101.3 kPa)	1.13	Mixed with water, ethanol, benzene, and toluene, slightly soluble in ethers, insoluble in petroleum ether



hexanedioic acid (99%), azelaic acid (98%), folic acid (FA), and ethylenediamine (EDA) were purchased from Sigma-Aldrich. NaOH (99%), NH_4F (99%), triethylene glycol (TEG)(GR), methyl cyanide (GR), and methanol (GR) were all purchased from Beijing Chemical Works. Deionized water was purified through a Milli-Q water purification system and the resistivity was 18.2 M Ω cm. All the chemicals were used as received without further purification.

2.2 Synthesis of $\text{NaYF}_4\text{:Yb, Er}$ UCNP s using diacid as a surfactant

The UCNP s were prepared using the traditional NaYF_4 as the matrix for the investigation of the reaction conditions. Typically, in a 100 mL three-necked flask, a total of 1 mmol $\text{LnCl}_3\cdot 6\text{H}_2\text{O}$ [0.78 mmol $\text{YCl}_3\cdot 6\text{H}_2\text{O}$, 0.2 mmol $\text{YbCl}_3\cdot 6\text{H}_2\text{O}$, and 0.02 mmol $\text{ErCl}_3\cdot 6\text{H}_2\text{O}$] were added, followed by the addition of 10 mmol diacid (PDA, HDA or AA) and 25 mL TEG. Here, the diacid was added in excess compared to the Ln element in order to avoid the cross-coordination between the two carboxyl groups and Ln ions and discharge from the other carboxyl group, hence improving the water solubility of the resulting NP s. After 30 min stirring under flowing argon at room temperature, this mixture was heated to 150 $^\circ\text{C}$ for 30 min to make a clear solution. It was then cooled down to room temperature, followed by an additional solution of 2.5 mmol NaOH and 4 mmol of NH_4F in 10 mL of methanol. The methanol was evaporated under heating at 80 $^\circ\text{C}$ in argon for 1 hour and then stirred at room temperature for another 1 hour. The reaction mixture was then heated up to a designed temperature (180–285 $^\circ\text{C}$) and stirred for a designed time and then cooled down to room temperature for the next mass weighing and purification process. Simply, the obtained NP s were cooled down to RT and then precipitated using excess methyl cyanide and isolated at 9000 rpm (a centrifugal force of 9000 g) for 10 min. The supernatant was poured off and the NP s in the bottom of the centrifuge tube were redispersed in water, precipitated using methyl cyanide, and isolated again at 9000 rpm (a centrifugal force of 9000g) for 10 min. This washing process was repeated twice. After the

purification, the NP s were stored as a dispersion in deionized water with a concentration of 20 mg mL $^{-1}$.

2.3 Surface modification of the UCNP s with FA

Considering the fact that the UCNP s and FA molecules were capped with negatively charged carboxylic groups, when the UCNP s and FA were mixed together in the same vessel, they could not combine with each other due to the electrostatic repulsive force. However, when the ethylenediamine-modified UCNP s were added into the FA solution, the UCNP s would readily be combined with the FA through the bridge link of ethylenediamine due to the electrostatic interaction. Experimentally, 10 mg of UCNP s was mixed with 5 mL of ethylenediamine for about 1 hour and then 0.5 mg of FA was added to the solution after another 1 hour of stirring. The mixed solution was then centrifuged at 9000 rpm for 20 min (three times) to purify the FA-modified UCNP s. The supernatant was withdrawn carefully and the NP s were dispersed in PBS solution (pH 7.4) for further use.

2.4 Cell imaging

For cell imaging, HeLa cells were incubated with 200 mg per L FA-EDA-UCNP s for 8 h at 37 $^\circ\text{C}$. The nuclei were then counterstained with 0.1 mg per L DAPI (4',6-diamidino-2-phenylindole) for 10 min at room temperature, followed by washing with PBS three times. Upconversion fluorescence imaging was then performed using a Nikon Inverted Microscope Eclipse Ti-U Main-Body (Nikon, Tokyo, Japan) equipped with a C2-SHS Scanner and Controller.

2.5 Characterization

Steady-state photoluminescence spectra were measured using an Ocean Optics spectrophotometer. The excitation wavelength was 980 nm. The FESEM images were taken on a Hitachi S-4800 scanning electron microscope with an acceleration voltage of 5 kV. The XRD patterns were obtained using a D8 FOCUS X-ray

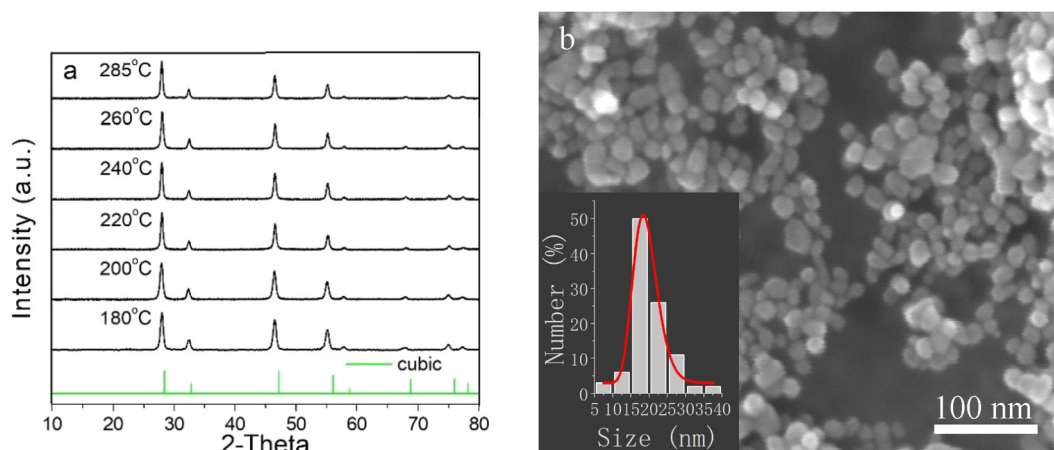


Fig. 1 XRD results of $\text{NaYF}_4\text{:Yb, Er}$ NP s prepared at 180 $^\circ\text{C}$, 200 $^\circ\text{C}$, 220 $^\circ\text{C}$, 240 $^\circ\text{C}$, 260 $^\circ\text{C}$, and 285 $^\circ\text{C}$ (a). The JCPDS file number for the standard cubic bulk structure is 77-2042. FE-SEM image of the $\text{NaYF}_4\text{:Yb, Er}$ UCNP s prepared at 285 $^\circ\text{C}$ (b). The histogram of the size distribution is shown in the inset.

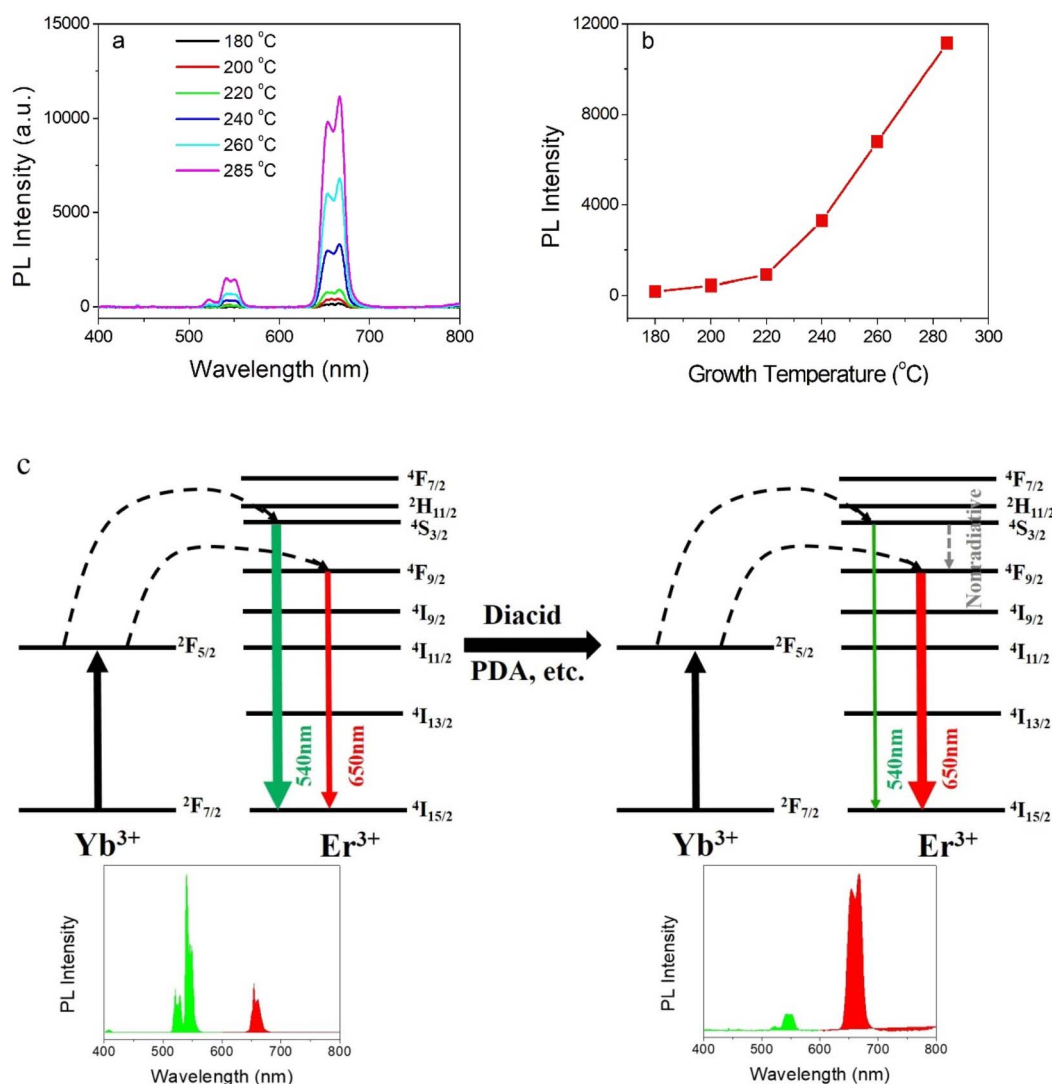


Fig. 2 Room-temperature UC luminescent spectra of NaYF₄:20%Yb, 2%Er NPs prepared at different growth temperature (a). Relative PL intensity of the two-photon (⁴F_{9/2}–⁴I_{15/2}) 650 nm UC emission of Er ions vs. the growth temperature (b). Mass concentration of the NPs was kept constant at 5 mg mL⁻¹. λ_{ex} = 980 nm. Schematic of energy level and UC luminescent spectra of the drop of the 540 nm green emission of NaYF₄:20%Yb, 2%Er NPs (c).

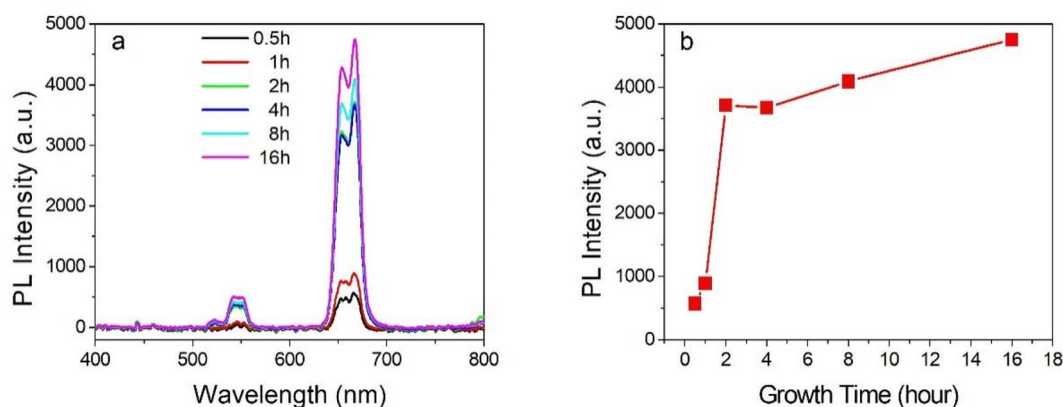


Fig. 3 Room-temperature UC luminescent spectra of NaYF₄:20%Yb, 2%Er NPs prepared at different growth times (a). Relative PL intensity of the two-photon (⁴F_{9/2}–⁴I_{15/2}) 650 nm UC emission of Er ions vs. the growth time (b). Mass concentration of the NPs was kept constant at 2 mg mL⁻¹. λ_{ex} = 980 nm.



diffractometer purchased from Bruker Company. Upconversion fluorescence imaging was performed using a Nikon Inverted Microscope Eclipse Ti-U MainBody (Nikon, Tokyo, Japan) equipped with C2-SHS Scanner and Controller.

3. Results and discussion

3.1 Influence of the synthesis temperature on the optical properties of the UCNPs

It is well known that lanthanide ions-doped NaYF_4 host lattices NPs have higher UC emission efficiency in comparison to Y_2O_3 and YVO_4 .^{21–23} Hence, we prepared $\text{NaYF}_4\text{:Yb, Er}$ UCNPs as a model system to verify the higher temperature synthesis in polar solution. As shown in Fig. 1, the XRD for the UCNPs presents the typical cubic phase crystal structure when they were prepared at different temperatures. Once the growth temperature was higher than 180 °C, the cubic phase structure appeared obviously, proving the formation of the crystals. As the temperature was increased from 180 to 285 °C, the intensities of the diffraction peaks were gradually increased (shown in Fig. S1, ESI†), which proves the thermodynamic crystallization process. This is in accordance with a previous report, which expounded that higher temperatures accelerate the crystallization

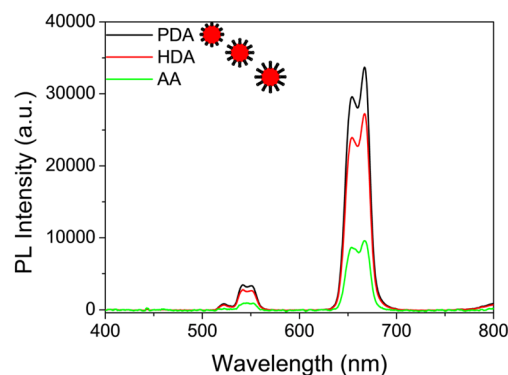
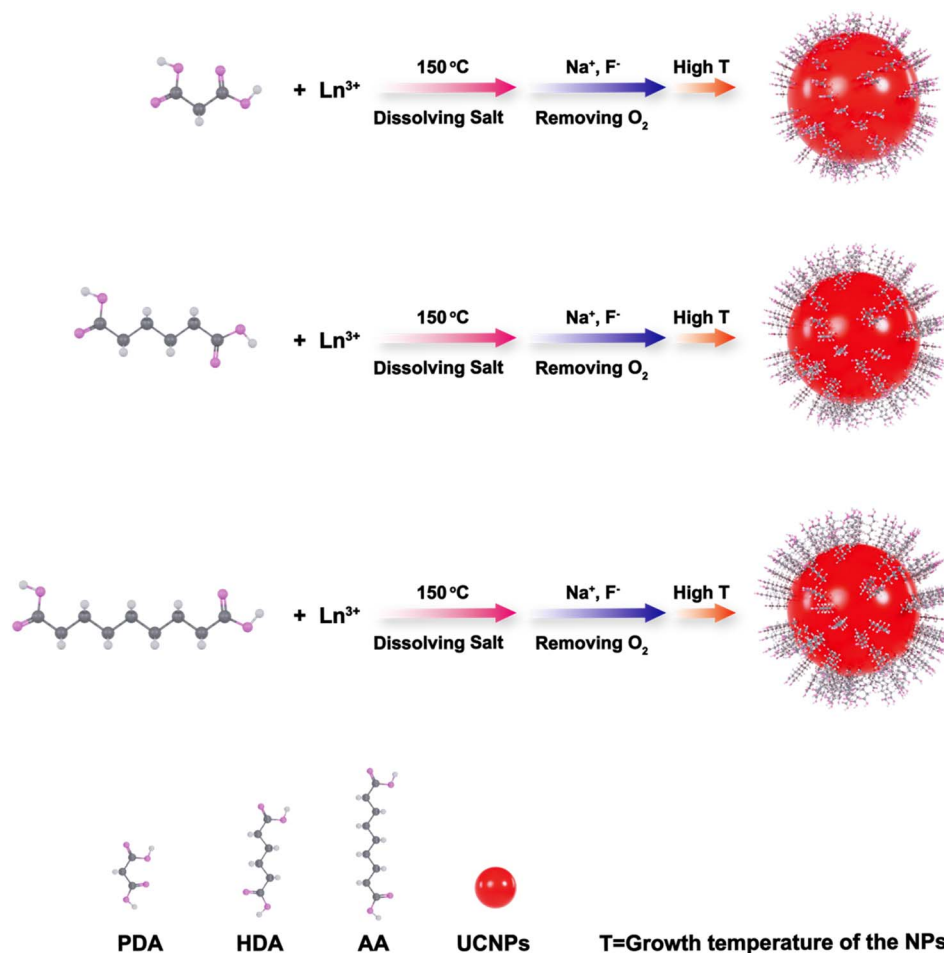


Fig. 4 Room-temperature UC luminescent spectra of $\text{NaYF}_4\text{:20%Yb, 2%Er}$ NPs prepared with different chain length diacid ligands. Mass concentration of the NPs was kept constant at 10 mg mL^{-1} . $\lambda_{\text{ex}} = 980 \text{ nm}$.

process.^{12,24} As shown in Fig. S1 (ESI)†, when the temperature was increased from 180 to 240 and 285 °C, the XRD diffraction peaks became sharper and stronger. This indicates that the nanoparticle growth is a strongly thermodynamics-dependent process.¹² Anyway, the growth temperature can be increased to



Scheme 1 Growth mechanisms of UCNPs grown at different diacid ligands.

285 °C, which is much higher than the traditional growth temperature (≤ 200 °C) in the polar solution reported previously.^{12,13,25} This is realized based on the introduction of diacid as a surfactant and TEG as a solvent. As shown in Fig. 1b, the FE-SEM image presents the spherical morphology of NaYF₄:Yb, Er UCNPs. After statistical analysis, the size of the prepared NaYF₄:Yb, Er UCNPs was found to be about 18 nm (see the size distribution in Fig. 1b), which is much smaller than that of the previous NaYF₄ UCNPs (mainly 100–900 nm) synthesized in the aqueous phase directly.¹²

From the traditional point of view, it is well accepted that elevating the growth temperature of nanocrystals tends to decrease the defects of the lattice and increase the luminescent emission efficiency. In this work, the experimental results coincide with this theory. As shown in Fig. 2a and b, when the growth temperature of the particles was elevated from 180 °C to 200 °C, 220 °C, 240 °C, 260 °C, and 285 °C, both the two-photon ($^4S_{3/2}$ – $^4I_{15/2}$) 540 nm and the two-photon ($^4F_{9/2}$ – $^4I_{15/2}$) 650 nm UC upconversion process of Er ions²⁶ were gradually increased. The decrease in the green emission vs. the red emission compared

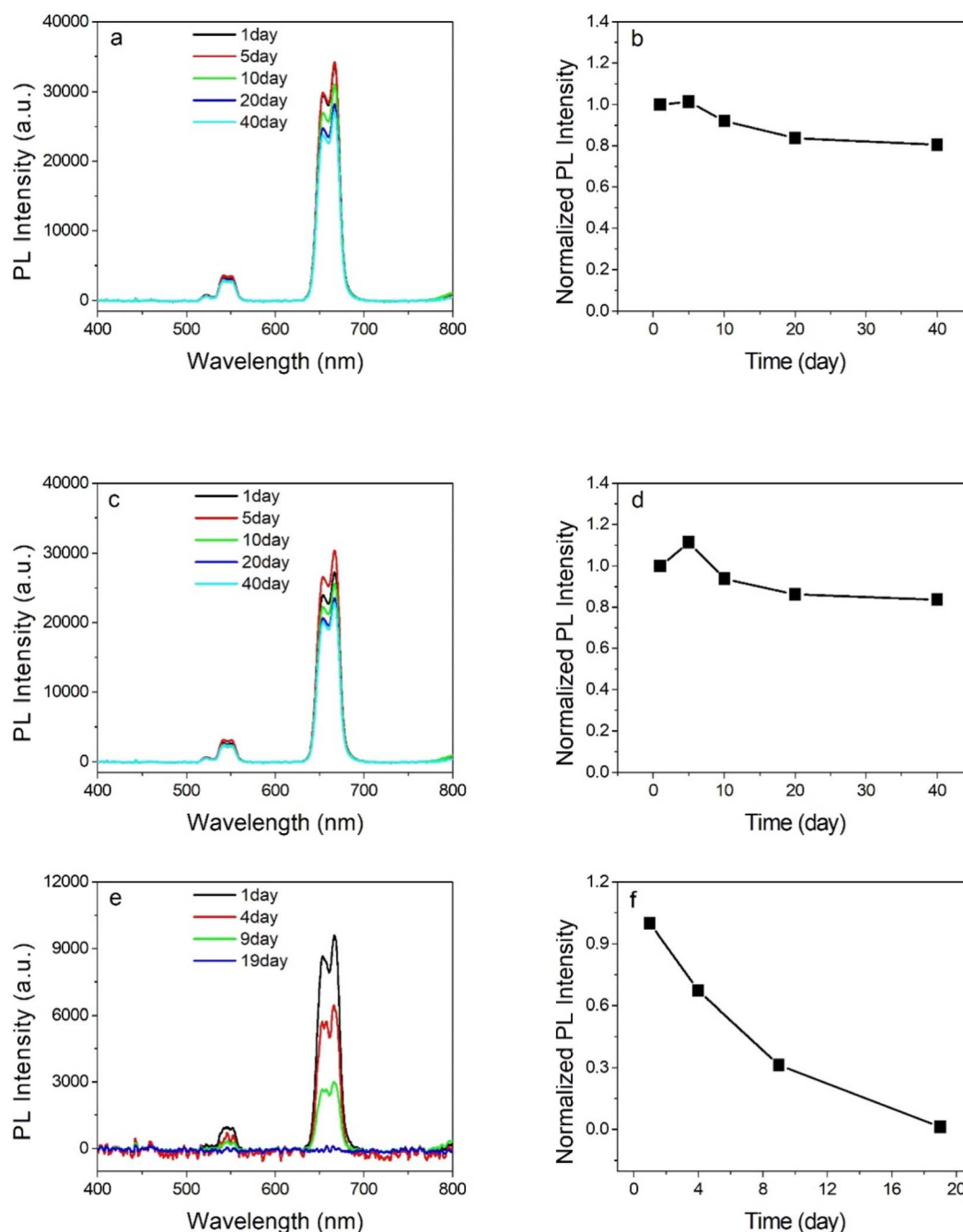


Fig. 5 Time evolution of room-temperature UC luminescent spectra and red emission intensity of NaYF₄:20%Yb, 2%Er NPs prepared with PDA (a and b), HDA (c and d) and AA (e and f) under natural position to compare the stability of the relative NPs. Mass concentration of the NPs was kept constant at 10 mg mL⁻¹. λ_{ex} = 980 nm.



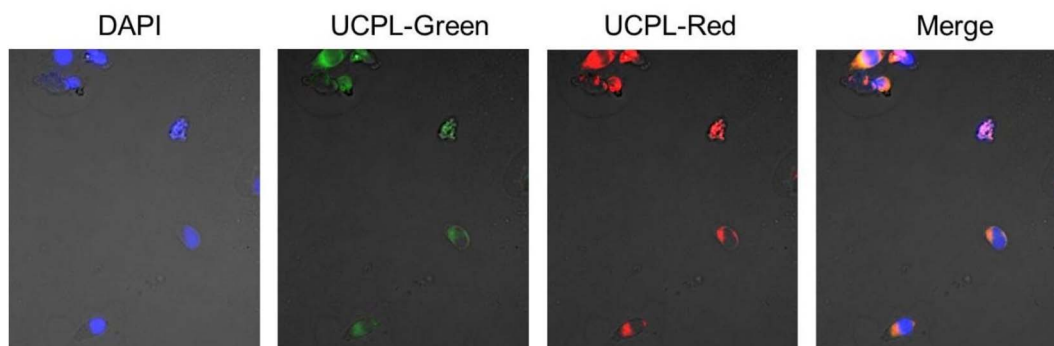


Fig. 6 UCPL images (green and red) of the FA-UCNPs under the excitation of 980 nm; the nuclei were stained by DAPI (blue image).

to the previous value of $\text{NaYF}_4\text{:Yb, Er}$ NPs synthesized in the oil phase is due to the abundant adsorption of the diacid onto the surface of the NPs, which will lead to an increase in the multiphonon nonradiative relaxation process from the $^2\text{H}_{11/2}$ and $^4\text{S}_{3/2}$ energy level transition to the $^4\text{F}_{9/2}$ energy level of Er ions and the ultimate increase in the green emission intensity. Therefore, it presents yellow upconversion luminescence in aqueous solution under the excitation of the 980 nm laser (shown in the inset of Fig. S1, ESI†). The energy schematic illustration of the decrease in the 540 nm green emission is shown in Fig. 2c.¹² Naturally, 285 °C was set as the optimal NP growth temperature for the next experimental investigation.

3.2 Influences of the synthesis time on the optical properties of the UCNPs

It is well known that the growth of the NPs is relative to the dynamic process. As a result, the relationship of the UC PL spectra vs. the growth time is measured. As shown in Fig. 3, as the growth time was increased from 0.5 hours to 16 hours, the UC PL intensity was increased rapidly from 0.5 to 2 hours and then an almost steady state was turned on. This proves that the NPs growth could be finished during 2 hours in the reaction conditions.

3.3 Influences of the carboxyl chain length of the diacid on the optical properties of the UCNPs

The influence of the carboxyl chain length of the diacid to the NPs' growth was also investigated by measuring the UC PL spectra at room temperature. The growth mechanism of the UCNPs at different carboxyl chain lengths of the diacid can be illuminated simply by the scheme shown in Scheme 1. As shown in Fig. 4, the UC PL intensity was in inverse ratio to the carbon chain length of the diacid. In this work, the relatively less carboxyl chain surfactant, PDA-coordinated UCNPs present a higher UC PL intensity. Furthermore, the short carboxyl chain diacid-stabilized UCNPs also showed better stability in polar solution. As shown in Fig. 5, the PDA and HDA-stabilized UCNPs maintained more than 80% PL intensity of the original UCNPs under 40 days of monitoring, and the UC PL intensity of AA-stabilized UCNPs will be quenched completely in about 20 days of monitoring. Compared with the traditional

method¹⁸ for obtaining the water-soluble UCNPs *via* the phase transfer of the original oil-phase UCNPs (shown in Scheme S1 and Fig. S2, ESI†), the stability of the UCNPs prepared directly in the polar solution by our method using PDA and HDA as the surfactant is much stronger than that of the UCNPs obtained by the phase-transfer method.

3.4 Upconversion luminescent cell imaging

To further testify the advantages of the synthesized NPs in the potential bio-applications, PL imaging testing on HeLa cells was performed. Notably, for a majority of previous works,²⁷ the employed UCNPs were oil-soluble, in which case, the phase transfer on NPs (from oil phase to water phase) is necessary to be carried out in advance, which makes the entire imaging process more onerous. However, in this work, benefiting from the relatively high synthesis temperature (*e.g.*, 285 °C), small-size and water-soluble $\text{NaYF}_4\text{:Yb, Er}$ UCNPs can be directly obtained in one step, which obviously simplifies the preparation process. As shown in Fig. 6, the cell nuclei were firstly stained by DAPI (a traditional dye, taken as a reference standard), and a blue imaging can be well observed. In the meantime, by introducing the UCNPs, high-quality UC images (with green and red light) can also be clearly obtained under the irradiation of a 980 nm laser (to increase the targeting effect of NPs to the cell, the UCNPs were combined with the FA through the bridge link of ethylenediamine due to the electrostatic interaction²⁸). The good overlap of these images indicates the success of the cellular internalization of the UCNPs as well as the potentiality of our material on bioimaging.

4. Conclusions

In conclusion, we have synthesized the water-soluble NaYF_4 UCNPs using diacid as a surfactant. The size of the prepared UCNPs can reach to be as small as 9 nm, which is the minimum size reported for the direct synthesis of water-soluble NaYF_4 UCNPs. The temperature-dependent nanocrystal growth mechanism and luminescent properties of UCNPs were explored deeply. The different chain length diacids were used in this work to prepare the water-soluble UCNPs in polar solution, and finally we found that the water-stability is inversely

proportional to the carbon chain length of the ligand. Propanedioic acid was proved to be an optimum surfactant in this work to prepare the most stable water-soluble UCNPs. Due to the abundant adsorption of the diacid onto the surface of the NaYF₄:20%Yb, 2%Er NPs, the nonradiative relaxation process from the ⁴S_{3/2} energy level transition to the ⁴F_{9/2} energy level of Er ions was strengthened. As a result, the green emission was weakened and the red emission was relatively enhanced ultimately. The resulting water-soluble UCNPs can also be successfully applied in upconversion luminescent cell imaging. This study opens new avenues for the synthesis of water-soluble UCNPs and provides more opportunities for their applications in bio-imaging, bio-detection, etc.

Data availability

All data in the main text and the ESI† are available from the corresponding authors on request.

Conflicts of interest

There are no conflicts to declare.

Acknowledgements

This work was supported by the Science and Technology Development Project of Jilin Province for Distinguished Young Scholars (No. 20240602011RC), the Transverse Research Project (No. 2023220001000025), the Jilin Provincial Development and Reform Commission (No. 2023C028-1), and the Science and Technology Development Project of Jilin Province (No. 20240404034ZP and No. YDZJ202201ZYTS260).

References

- 1 R. R. Deng, F. Qin, R. F. Chen, W. Huang, M. H. Hong and X. G. Liu, *Nat. Nanotechnol.*, 2015, **10**, 237–242.
- 2 D. M. Yang, P. A. Ma, Z. Y. Hou, Z. Y. Cheng, C. X. Li and J. Lin, *Chem. Soc. Rev.*, 2015, **44**, 1416–1448.
- 3 S. H. Bi, Z. M. Deng, J. Q. Huang, X. W. Wen and S. J. Zeng, *Adv. Mater.*, 2023, **35**, 2207038.
- 4 J. Zuo, L. P. Tu, Q. Q. Li, Y. S. Feng, I. Que, Y. L. Zhang, X. M. Liu, B. Xue, L. J. Cruz, Y. L. Chang, H. Zhang and X. G. Kong, *ACS Nano*, 2018, **12**, 3217–3225.
- 5 W. F. Yang, X. Y. Li, D. Z. Chi, H. J. Zhang and X. G. Liu, *Nanotechnology*, 2014, **25**, 482001.
- 6 S. W. Wu, G. Han, D. J. Milliron and P. J. Schuck, *Proc. Natl. Acad. Sci. U. S. A.*, 2009, **106**, 10917–10921.
- 7 J. Zhou, Z. Liu and F. Y. Li, *Chem. Soc. Rev.*, 2012, **41**, 1323–1349.
- 8 L. Palanikumar, M. Kalmouni, T. Houhou, O. Abdullah, L. Ali, R. Pasricha, R. Straubinger, S. Thomas, A. J. Afzal, F. N. Barrera and M. Magzoub, *ACS Nano*, 2023, **17**, 18979–18999.
- 9 S. Chen, A. Z. Weitemier, X. Zeng, L. M. He, X. Y. Wang, Y. Q. Tao, A. J. Y. Huang, Y. Hashimoto, M. Kano, H. Iwasaki, L. K. Parajuli, S. Okabe, D. B. L. Teh, A. H. All, I. Tsutsui-Kimura, K. F. Tanaka, X. G. Liu and T. J. McHugh, *Science*, 2018, **359**, 679–683.
- 10 A. D. Ostrowski, E. M. Chan, D. J. Gargas, E. M. Katz, G. Han, P. J. Schuck, D. J. Milliron and B. E. Cohen, *ACS Nano*, 2012, **6**, 2686–2692.
- 11 Z. B. Luo, Q. G. Qi, L. J. Zhang, R. J. Zeng, L. S. Su and D. P. Tang, *Anal. Chem.*, 2019, **91**, 4149–4156.
- 12 J. W. Zhao, Y. J. Sun, X. G. Kong, L. J. Tian, Y. Wang, L. P. Tu, J. L. Zhao and H. Zhang, *J. Phys. Chem. B*, 2008, **112**, 15666–15672.
- 13 J. W. Zhao, X. M. Liu, D. Cui, Y. J. Sun, Y. Yu, Y. F. Yang, C. Du, Y. Wang, K. Song, K. Liu, S. Z. Lv, X. G. Kong and H. Zhang, *Eur. J. Inorg. Chem.*, 2010, 1813–1819.
- 14 F. Wang, Y. Han, C. S. Lim, Y. H. Lu, J. Wang, J. Xu, H. Y. Chen, C. Zhang, M. H. Hong and X. G. Liu, *Nature*, 2010, **463**, 1061–1065.
- 15 L. L. Liang, Y. M. Liu, C. H. Bu, K. M. Guo, W. W. Sun, N. Huang, T. Peng, B. Sebo, M. M. Pan, W. Liu, S. S. Guo and X. Z. Zhao, *Adv. Mater.*, 2013, **25**, 2174–2180.
- 16 H. S. Qian and Y. Zhang, *Langmuir*, 2008, **24**, 12123–12125.
- 17 H. X. Mai, Y. W. Zhang, R. Si, Z. G. Yan, L. D. Sun, L. P. You and C. H. Yan, *J. Am. Chem. Soc.*, 2006, **128**, 6426–6436.
- 18 Q. B. Zhang, K. Song, J. W. Zhao, X. G. Kong, Y. J. Sun, X. M. Liu, Y. L. Zhang, Q. H. Zeng and H. Zhang, *J. Colloid Interface Sci.*, 2009, **336**, 171–175.
- 19 W. Lin, K. Fritz, G. Guerin, G. R. Bardajee, S. Hinds, V. Sukhovatkin, E. H. Sargent, G. D. Scholes and M. A. Winnik, *Langmuir*, 2008, **24**, 8215–8219.
- 20 N. J. J. Johnson, N. M. Sangeetha, J. C. Boyer and F. C. J. M. van Veggel, *Nanoscale*, 2010, **2**, 771–777.
- 21 G. Y. Chen, H. L. Qiu, P. N. Prasad and X. Y. Chen, *Chem. Rev.*, 2014, **114**, 5161–5214.
- 22 F. Wang and X. G. Liu, *J. Am. Chem. Soc.*, 2008, **130**, 5642–5643.
- 23 F. Wang, J. Wang and X. G. Liu, *Angew. Chem., Int. Ed.*, 2010, **49**, 7456–7460.
- 24 J. Luo, Q. H. Zhang and S. L. Suib, *Inorg. Chem.*, 2000, **39**, 741–747.
- 25 Y. J. Sun, H. J. Liu, X. Wang, X. G. Kong and H. Zhang, *Chem. Mater.*, 2006, **18**, 2726–2732.
- 26 Q. H. Zeng, B. Xue, Y. L. Zhang, D. Wang, X. M. Liu, L. P. Tu, H. F. Zhao, X. G. Kong and H. Zhang, *CrystEngComm*, 2013, **15**, 4765–4772.
- 27 L. Xia, X. G. Kong, X. M. Liu, L. P. Tu, Y. L. Zhang, Y. L. Chang, K. Liu, D. Z. Shen, H. Y. Zhao and H. Zhang, *Biomaterials*, 2014, **35**, 4146–4156.
- 28 Q. H. Zeng, Q. Li, W. Y. Ji, B. Xue and J. Song, *Sci. Rep.*, 2016, **6**, 26534.

